

Optical and electrical properties of pulsed laser annealed thin Si films

J. Bischof, J. Boneberg, C.H. Dorfmueller, M. Keil, M. Lux-Steiner, P. Leiderer
Fakultät für Physik, Universität Konstanz, 78434 Konstanz, Germany

ABSTRACT

Thin Si films used for solar energy purposes are commonly treated by relatively slow thermal annealing on a time scale of seconds to obtain the proper electrical behavior. We investigate a different approach, in which the films are annealed and/or molten by a frequency doubled Q-switched Nd:YAG laser pulse on a nanosecond time scale. We studied thin polycrystalline Si films of thickness between 43 nm and 250 nm on fused silica and on sapphire substrates. The different thermal conductivities of these substrates lead to different quench rates for the molten Si films. The optical and electrical properties of the Si films were systematically characterized during, respectively after the various annealing conditions. In addition we monitored the solidification process in situ by time-resolved optical measurements. At low energy densities the film is not completely molten by the laser pulse and resolidification takes place at the moving liquid-solid interface. Above a thickness-dependent threshold energy density complete melting is observed and nucleation in the supercooled melt prevails. In the latter case Sameshima and Usui¹ showed that amorphization can be observed for Si films on fused silica up to thicknesses of 36 nm. We found that Si films on sapphire even with a thickness of 80 nm can be amorphized. The reproducible threshold values suggest the possibility of lateral structuring.

1. INTRODUCTION

In thin film technology of semiconductors different approaches can be taken to remove defects in the crystal structure², e.g. after production on substrates or ion implantation. This can be achieved for example by thermal annealing in a furnace, electron beam processing and laser annealing. In this work we report on pulsed laser annealing of thin Si films on fused silica and sapphire substrates. Time resolved optical measurements provide a powerful tool to get insight into the dynamics during the annealing process. We show that depending on the laser energy density and substrate material different electrical, optical and structural properties can be achieved. These can be associated with different dynamic scenarios.

2. EXPERIMENT

The samples used were polycrystalline Si (pc-Si) films with various thicknesses in the range between 40 nm and 250 nm: on 1 mm fused silica and 0.5 mm sapphire substrates. The Si films were deposited by CVD technique at a substrate temperature of 600°C. The reacting gas consisted of 99.5% SiH₄ and 0.5% PH₃, the latter being added in order to shift the electrical conductivity into a more suitable range. By spectral ellipsometric measurements the crystallinity was proven to be usually more than 85%.

The annealing laser was a frequency doubled Q-switched Nd:YAG laser with a pulse length of 7 ns full width at half-maximum and a beam profile close to TEM₀₀. The Nd:YAG pulse, incident nearly perpendicular to the surface, was only mildly focused to a spot diameter of about 1 mm. To investigate the dynamics during annealing we measured the reflectivity of two s-polarized continuous wave lasers⁶ (Fig. 1). A HeNe laser (633 nm, 8 mW) was used for measuring the reflectivity from the free surface of the Si film at an angle of incidence of 45°, and an Ar⁺ laser (488 nm, 15 mW) probed the reflectivity from the film-substrate interface, incident at 30° onto the back of the substrate. These two probe lasers were focused to a 1/e diameter smaller than 20 μm onto the surface of the Si film and onto film-substrate interface, respectively. There the overlap of both spots was better than 90%. In this manner variations

in the much wider pulse laser intensity profile across the probe laser foci are negligible. The reflected and transmitted intensities of the probe lasers were detected by pin diodes with risetimes less than 1 ns and registered by fast digital storage oscilloscopes (HP54111D and HP54510A). Interference filters in front of the pin diodes were used to suppress contributions of the annealing pulse to the measured signals.

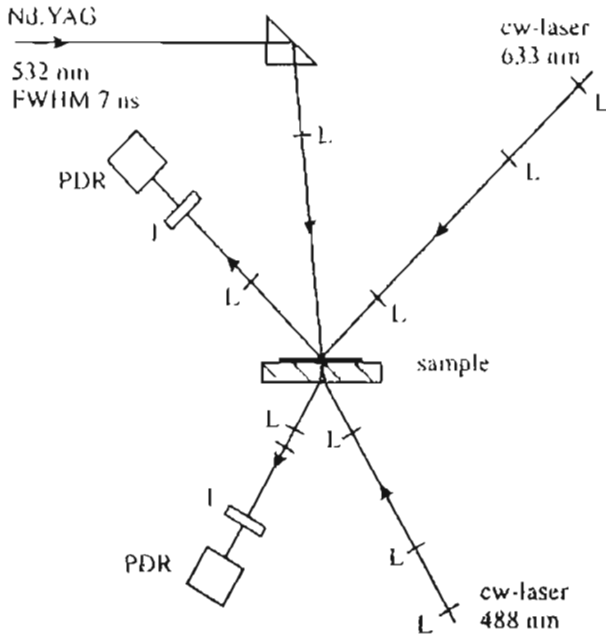


Figure 1: Schematic set-up of the experiment to investigate the dynamics during laser annealing. I: interference filter; L: lens; PDR: pin photodiode for reflection measurements.

3. RESULTS AND DISCUSSION

The experimental set-up shown in Fig. 1 allows for in situ monitoring the influence of the annealing laser on the Si film at the location of the probe lasers. Thereby, depending on the energy density of annealing pulses, three different scenarios can be distinguished for all Si film thicknesses and substrates: with increasing energy density first heating without melting, then partial melting from the surface and finally complete melting of the thin films take place. Since the annealing pulse has a nearly gaussian beam profile, complete melting of the Si film in the middle of the spot leads to partial melting at outer areas. Microscopic pictures of the optical appearance for different film thicknesses and substrates are shown in Fig. 2.

Completely molten and incompletely molten regions due the radial decrease in the pulsed laser intensity can be distinguished as concentric areas of different brightness corresponding to crystalline and amorphous (see section 3.3) structure, respectively. The details of the resolidification process leading to these structurally different modifications sensitively depend on Si film thickness, substrate material and laser energy density.

3.1 Thresholds

Time-resolved reflectivity and transmissivity measurements of the probe lasers with ns resolution allow to distinguish between heating, incomplete and complete melting at the location of the probe lasers. Since the optical constants are temperature dependent², heating results in a change of the absorptivity and of the interference conditions for the reflected and transmitted intensities.

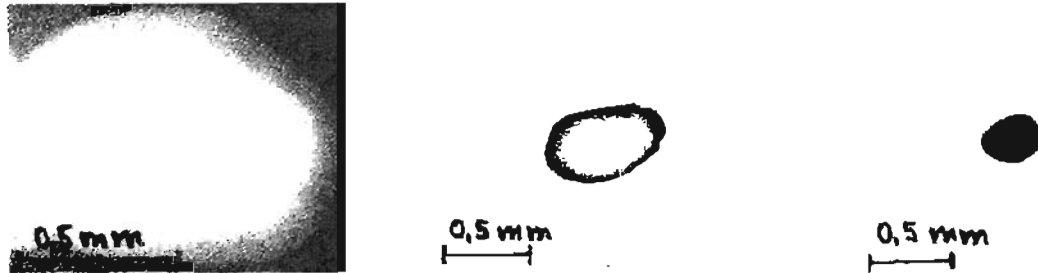


Figure 2: Pictures of laser annealed spots taken with an optical transmission microscope. The frame size of the pictures corresponds to a size of $2 \times 1.5 \text{ mm}^2$ for the first photograph and to $1 \times 0.7 \text{ mm}^2$ for the other two. Different properties of the areas upon heating, incomplete and complete melting can be distinguished and characterized: a) After annealing the whole film is polycrystalline. The three concentric regions of different brightness correspond to completely molten, incompletely molten and heated areas, respectively, and reflect the pulse laser shape. The Si film on fused silica was 248 nm thick (annealing laser energy density of 475 mJ/cm^2). b) At this smallest investigated thickness of the original pc-Si on fused silica an amorphous ring at the rim of the completely molten region appears. 50 nm Si film on fused silica (300 mJ/cm^2) c) The whole inner, completely molten region solidifies into the amorphous phase (a-Si). 80 nm Si film on sapphire (360 mJ/cm^2 , just above the threshold for complete melting).

The transition from heating to melting can be resolved easily because of the metallic properties of molten silicon resulting in a high reflectivity and a transmissivity near zero. The absorption length in liquid Si is about 10 nm^4 . With one probe laser reflected at the free surface and one reflected at the film-substrate interface, we can thus distinguish between partial and complete melting of Si films (see 3.2).

In Fig. 3 thresholds for the various processes and different Si film thicknesses on the two substrates are given. The typical errors in the energy density and in the film thickness are 5% and 10%, respectively. Starting at low energy densities the Si film is heated until at the threshold E_{incomp} partial melting from the free surface is first observed. For energy densities between E_{comp} and E_{damage} the film melts completely. Here E_{damage} is the energy density where the pulsed laser causes irreversible damage on the Si film.

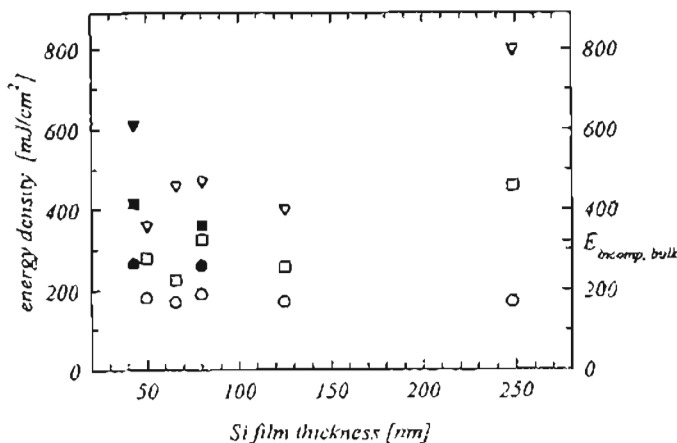


Figure 3: Thresholds in the energy density of the pulsed laser for various thicknesses of Si films on fused silica (open symbols) and sapphire (filled symbols) substrates. Circles and squares denote the threshold energy densities E_{incomp} and E_{comp} for incomplete and complete melting. Triangles denote the threshold energy density E_{damage} where irreversible damage results. Thresholds for crystalline bulk Si (100) are: $E_{\text{incomp}} = 320 \text{ mJ/cm}^2$ and $E_{\text{damage}} = 2400 \text{ mJ/cm}^2$.

Note that within the experimental error of 5 % the threshold E_{incomp} for different thicknesses of Si films on the same substrate material is constant. As expected, for films on sapphire this threshold is higher than on fused silica. This reflects the higher thermal conductivity of sapphire ($22 \text{ Wm}^{-1}\text{K}^{-1}$ at 320 K) compared to fused silica ($1.4 \text{ Wm}^{-1}\text{K}^{-1}$ at 320 K). In addition all the various thresholds in the energy density for Si films on sapphire are higher than those on fused silica indicating that thermal properties of the substrate play a dominant role in the annealing behavior.

Even for the sapphire substrate, however, the thresholds are distinctly lower than the ones of crystalline bulk Si (100) (thermal conductivity of $152 \text{ Wm}^{-1}\text{K}^{-1}$ at 320 K), where $E_{\text{incomp}} = 320 \text{ mJ/cm}^2$ and $E_{\text{damage}} = 2400 \text{ mJ/cm}^2$ ⁵.

For energy densities below E_{comp} the whole irradiated region is polycrystalline after annealing. Above E_{comp} , on the other hand, amorphization of the Si film takes place under certain conditions. For Si films on fused silica this formation of the amorphous phase is found only at the outer rim of the completely molten region for the thinnest investigated film (thickness of 50 nm). The portion of amorphized to the whole completely molten area decreases with increasing energy density.

For Si films on sapphire amorphization always took place upon complete melting for the investigated films with 80 nm and 43 nm thickness.

3.2 Resolidification dynamics

In addition to the determination of the energy density thresholds, time-resolved measurements enable one to extract information on the dynamics of the laser annealing process.

a) Si films on fused silica

In Fig. 4 three curves for the time-depending reflectivity $R(t)$ of the HeNe laser at the free surface of a 80 nm thick Si film on fused silica are shown. The top curve 4a represents the case of incomplete melting of the Si film. The two other curves show $R(t)$ upon complete melting with different energy densities. On a time scale shorter than $1 \mu\text{s}$ the starting values of the reflectivity were reached for all cases.

Si films with a thickness of 125 nm on fused silica have been studied in detail in an earlier investigation ⁶. They show the same dynamic behavior. The model for the solidification processes presented in this paper will be shortly summarized here:

i) In the case of incomplete melting (Fig. 4a) the reflectivity of the HeNe laser reaches the value for liquid Si of $R \sim 80\%$. As long as the liquid layer is present at the surface with a thickness greater than the absorption length of about 10 nm ⁴ this value remains nearly constant. Due to the heat flux into the substrate resolidification takes place at the solid-liquid interface and proceeds to the free surface. This leads to a sharp decrease in $R(t)$ as soon as this boundary reaches the penetration depth of the probe laser.

ii) Upon complete melting (Fig. 4b,c) nucleation in the undercooled melt takes place. Typical quench rates can exceed 10^{10} Ks^{-1} and thus undercooling can reach $T_m/2$ ⁸, where $T_m = 1685 \text{ K}$ is the melting temperature of Silicon. The latent heat released upon resolidification leads to a double plateau in the reflectivity curve, furthermore it was deduced from the $R(t)$ curves that a transient formation of amorphous phase should take place during the cool-down for a short time interval of some 10 ns.

From the work of Stiffler et al. ⁸ as well as from this resolidification model it was inferred that for higher quench rates the films could permanently resolidify in the amorphous phase. These higher quench rates can be reached either by thinner films or by substrates with higher thermal conductivity, e.g. sapphire.

b) Si films on sapphire

Fig. 5 shows the time-resolved measurements during annealing of a 80 nm thick Si film on sapphire.

i) The top curve 5a corresponds as in Fig. 4a to incomplete melting of the Si film. The most obvious difference between these two measurements is the much more shorter time scale on which the reflectivity

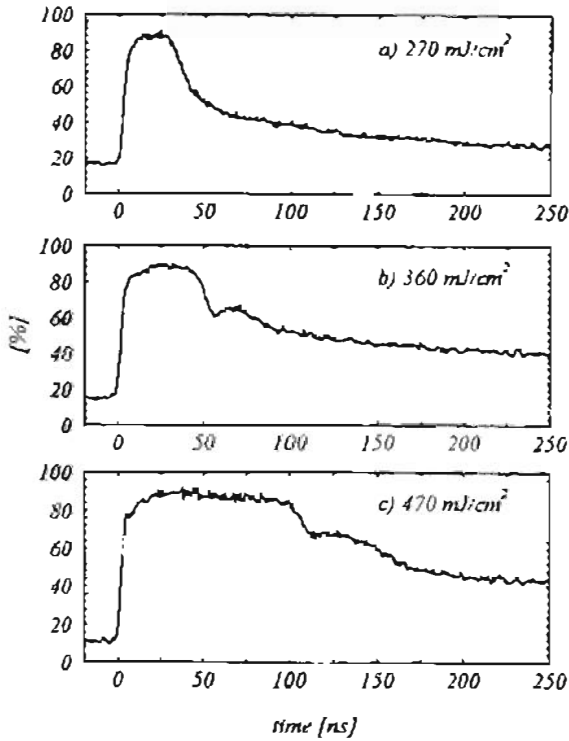


Figure 4: Time-resolved reflectivity of the free surface at $\lambda = 633 \text{ nm}$ during laser annealing of a 80 nm thick Si film on fused silica at different laser energy densities. The laser pulse hits the film surface at $t = 0 \text{ ns}$.

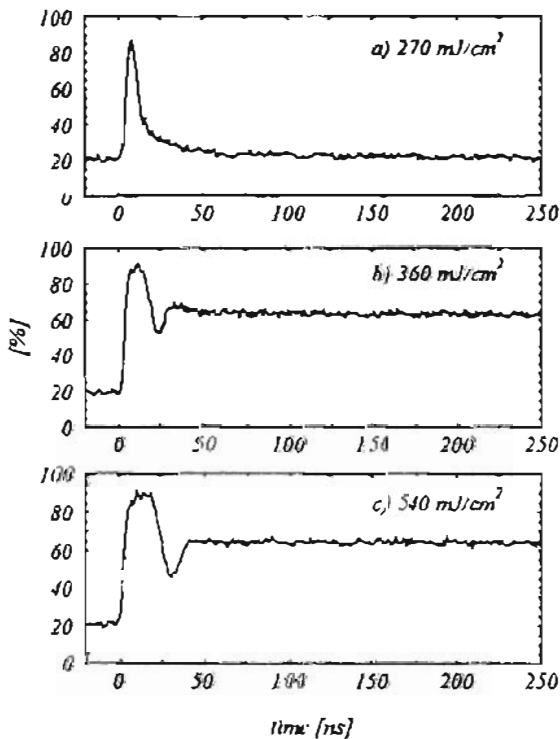


Figure 5: Time-resolved reflectivity of the free surface at $\lambda = 633 \text{ nm}$ during laser annealing of 80 nm Si film on sapphire at different laser energy densities.

goes back to the original value for the Si film on sapphire in spite of the same energy density. This is due to the higher thermal conductivity of sapphire compared to fused silica.

The resulting areas were always polycrystalline after annealing as in the case of Si films on fused silica.

ii) Fig. 5b,c show $R(t)$ in the case of complete melting of the Si films. Compared to Fig. 4b,c again the shorter time scale on which the reflectivity reaches an stable value is evident. It is also obvious that the values before and after the annealing are different. The difference occurred always upon complete melting of the Si film and reached always the same end value of $R(t)$.

The spots could be clearly distinguished even by the naked eye, appearing as darker brown areas. From the ellipsometric measurements (see 3.3) it was determined that the amorphous phase was generated.

This observed amorphization thus supports the model of the resolidification process given above.

3.3 Optical and electrical properties

Preliminary electrical measurements were made by directly contacting two needle-shaped tips on the film. The contact was checked to be ohmic in all cases. Care was taken to adjust the same distance between the tips in order to facilitate a comparison of resistances for different structures. Compared to the as-deposited film the resistance of the polycrystalline resolidified regions was lower by a factor of ten. For the amorphized regions on sapphire substrates the resistance was at least three orders of magnitude higher than that of the untreated film.

The optical constants extracted from fits to spectroscopic ellipsometric measurements are shown in Fig. 6.

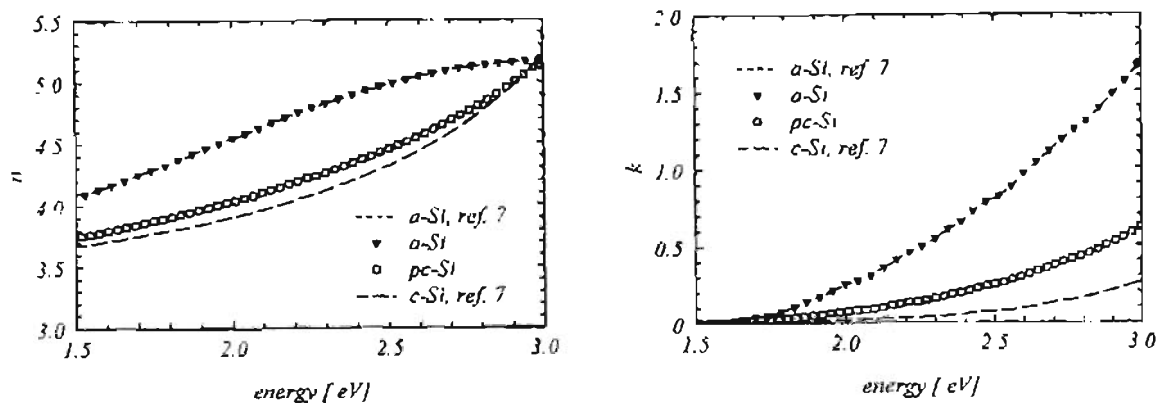


Figure 6: Refractive index n and extinction coefficient k versus photon energy. The data points for the as-deposited Si ($pc-Si$) and for the amorphous spots ($a-Si$) were extracted from fits to spectroscopic ellipsometric measurements on the respective areas on a 80 nm thick film on sapphire substrate. For comparison the optical constants taken from Ref. 7 for single crystalline and amorphous silicon are shown.

For the as-deposited Si films the values of the refractive index are close to those of the single crystalline material ⁷ also shown in Fig. 6. The extinction coefficient, however, differs significantly which can be attributed to disorder effects due to grain boundaries.

Resolidification of completely molten regions of the 80 nm thick Si film on sapphire yields spots with high absorption (see Fig. 2). The resulting optical constants of the fits to the spectroscopic ellipsometric measurements are in excellent agreement with the values for amorphous Si given by Aspnes and coworkers ⁷. We thus conclude that at these spots the material resolidified in the amorphous phase.

4. SUMMARY

In summary, we have presented properties of laser-annealed Si films with various thicknesses on fused silica and sapphire substrates. The measurements show that ns-resolved optical investigations are a powerful tool to give insight into the involved processes and thus control the resulting electrical, optical and structural properties.

It has been demonstrated that the resulting properties can be influenced with respect to different aspects:

i) Structural changes from the crystalline phase into the amorphous phase which result in different optical properties.

ii) Concerning the electrical resistance compared to the as-deposited Si film a lowering upon incomplete melting of the Si films, independent of the investigated substrate material and the Si film thickness, as well as a higher resistance upon amorphization can be reached.

Since the threshold values for the various processes were quite reproducible, lateral structuring in the optical and electrical properties appears feasible.

Experimentally we have determined thresholds in the energy density of the annealing laser for incomplete melting, complete melting and damaging of the Si films with different thicknesses.

Sameshima and Usui¹ found amorphization of the whole annealed areas after complete melting for Si films on fused silica having thicknesses in the range between 6 nm and 24 nm. They observed for Si films up to 36 nm that amorphization still plays a role, but in their Raman spectra already clear features of a partially crystalline phase occur. We report for the first time that complete amorphization by laser annealing on sapphire substrates up to Si film thicknesses of 80 nm can be achieved. Thus on sapphire it is possible to amorphize films which are thicker by at least a factor of three compared to those on fused silica.

5. ACKNOWLEDGEMENTS

The authors wish to thank T. Palberg for fruitful discussions and G. Kragler for her help with the ellipsometric measurements. This work was supported by Zentrum II für Energieforschung at the University of Konstanz.

6. REFERENCES

1. T. Sameshima, S. Usui, "Pulsed laser-induced melting followed by quenching of silicon films", *J. Appl. Phys.*, 74, 11; pp. 6592-6598, 1993
2. J.M. Poate, J.W. Mayer, "Laser Annealing of semiconductors", Academic Press Inc., New York, 1982
3. G.E. Jellison, F.A. Mondine, "Optical absorption of silicon between 1.6 and 4.7 eV at elevated temperatures", *Appl. Phys. Lett.*, 41, 2, pp. 180-182, 1982
4. G.E. Jellison, D.H. Lowndes, "Measurements of the optical properties of liquid silicon and germanium using nanosecond time resolved ellipsometry", *Appl. Phys Lett.*, 51, 5, pp. 352-354, 1987
5. J. Boneberg, O. Yavas, B. Mierswa, P. Leiderer, "Dynamics of the optical parameters of molten silicon during nanosecond laser annealing", *Lasers in Microelectronic Manufacturing*, Proceedings of SPIE Vol. 1598, pp. 84-90, 1991
6. J. Boneberg, J. Nedelcu, H. Bender, P. Leiderer, "Dynamics of the solidification of laser-annealed Si thin films", *Materials Science and Engineering*, A173, pp. 347-359, 1993
7. D.E. Aspnes, A.A. Studna, E. Kinsbron, "Dielectric properties of heavily doped crystalline and amorphous silicon from 1.5 to 6.0 eV", *Phys. Rev. B*, 29, 2, pp. 786-779, 1984
8. S.R. Stiffler, M.O. Thompson, P.S. Peercy, "Transient nucleation following pulsed-laser melting of thin silicon films", *Phys. Rev. B*, 43, pp. 9851-9855, 1991